Graphene for Controlled and Accelerated Osteogenic Differentiation of Human Mesenchymal Stem Cells

Tapas R. Nayak,[†,▽] Henrik Andersen,[‡,▽] Venkata S. Makam,[†] Clement Khaw,[§] Sukang Bae,[⊥] Xiangfan Xu,[‡] Pui-Lai R. Ee,[†] Jong-Hyun Ahn,[⊥,∥] Byung Hee Hong,[⊥,¶] Giorgia Pastorin,[†,#,▲,*] and Barbaros Özyilmaz[‡,#,▲,*]

[†]Department of Pharmacy, National University of Singapore, 3 Science Drive 2, Singapore 117543, [‡]Graphene Research Center and Department of Physics, National University of Singapore, 2 Science Drive 3, Singapore 117542, [§]Nikon Imaging Centre, No. 11 Biopolis Way, Helios Building, Singapore 138677, [⊥]SKKU Advanced Institute of Nanotechnology (SAINT) and Center for Human Interface Nano Technology (HINT), [∥]School of Advanced Materials Science and Engineering, and [¶]Department of Chemistry, Sungkyunkwan University, Suwon 440-746, Korea, [#]NUS Graduate School for Integrative Sciences and Engineering, Centre For Life Sciences (CeLS), 28 Medical Drive, #05-01, Singapore 117456, and [▲]NanoCore, Engineering Block A, EA, Level 4, Room No. 27, Faculty of Engineering, National University of Singapore, Singapore 117576. [▽]These authors contributed equally to this work.

ABSTRACT Current tissue engineering approaches combine different scaffold materials with living cells to provide biological substitutes that can repair and eventually improve tissue functions. Both natural and synthetic materials have been fabricated for transplantation of stem cells and their specific differentiation into muscles, bones, and cartilages. One of the key objectives for bone regeneration therapy to be successful is to direct stem cells' proliferation and to accelerate their differentiation in a controlled manner through the use of growth factors and osteogenic inducers. Here we show that graphene provides a promising biocompatible scaffold that does not hamper the proliferation of human mesenchymal stem cells (hMSCs) and accelerates their specific differentiation into bone cells. The differentiation rate is comparable to the one achieved with common growth factors, demonstrating graphene's potential for stem cell research.

KEYWORDS: graphene · mesenchymal stem cells · cell differentiation · bone · osteogenesis

Human mesenchymal stem cells (hMSCs) are critical for numerous groundbreaking therapies in the field of regenerative medicine. A myriad of environmental factors including their interaction with soluble growth factors, extracellular matrices, and neighboring cells are crucial for their survival, proliferation, and differentiation into specific lineages.[1−3] One of the main goals of tissue engineering is to control these factors by creating physical and chemical microenvironments designed to guide the ultimate fate of stem cells. Materials with different elasticity, rigidity, and texture have been extensively investigated for this purpose. Stem cell scaffolds, which can be both 2D and 3D in nature, have been fabricated to mimic the intrinsic characteristics of natural substrates such as muscle, bone, and cartilage.[4−6] Recently, the lithographic patterning of suitable surfaces such as polydimethylsiloxane (PDMS),[7] polymethyl methacrylate (PMMA),[8] self-assembled titanium dioxide (TiO_2)[9] rod arrays, and functionalized carbon nanotubes[10] has been explored. While there have been tremendous advances in this field, many challenges still remain. In particular, in the field of bone tissue engineering, almost all artificial materials require the administration of multiple growth factors to promote hMSC differentiation. In addition, many approaches face challenges when it comes to scalability and compatibility with implants. For example, an alloplastic (nonbiologic) material under mechanical strain may not perform in a similar way as the neighboring host bone tissues, ensuing in structural defects at the implant site or inflammatory responses in the original bone, as observed in stress shielding.[11] Also, bioactive implants still face limitations in terms of potential pathogenic infections, low availability, and high costs. Graphene[12] may provide an elegant solution to some of these challenges. Being only one atom thick, it introduces the least amount of artificial material possible and has a large number of remarkable properties.[13] In the context of tissue engineering, its mechanical properties are likely to play a key role: graphene has the highest Young's modulus (0.5−1 TPa) among any known material, yet it is not brittle.[14,15] Graphene can be transferred onto any flat or irregular-shaped surface, and graphene-coated, flexible, supporting substrates can be easily bent into any shape required.[16]

* Address correspondence to barbaros@nus.edu.sg, phapg@nus.edu.sg.

Received for review February 7, 2011 and accepted April 29, 2011.

Published online April 29, 2011
10.1021/nn200500h

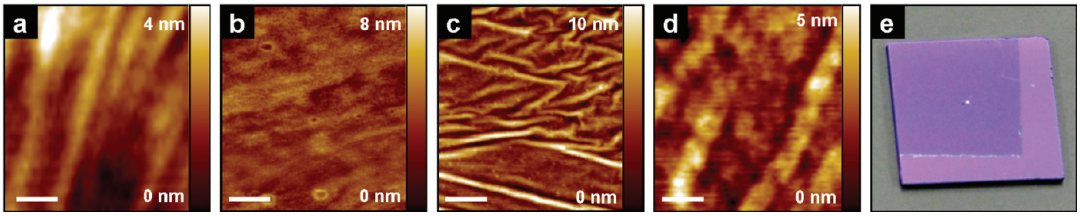

Figure 1. Graphene onto different substrates. AFM of graphene on (a) Si/SiO_2, (b) glass slide, (c) PET film, and (d) PDMS. Scale bars are 200 nm. (e) Optical image of 1 cm × 1 cm, partially graphene coated Si/SiO_2 chip, showing the graphene boundary.

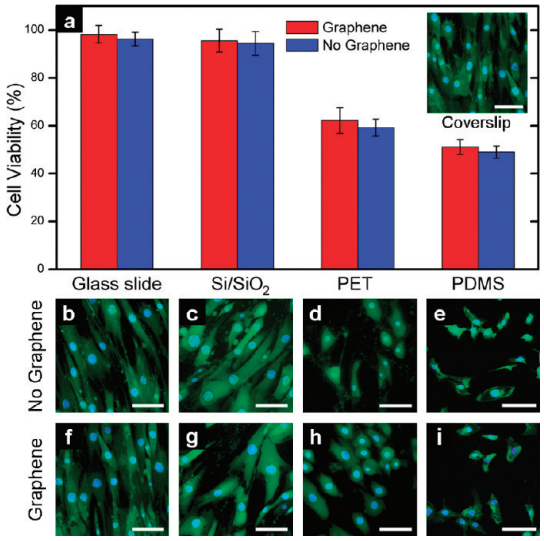

Figure 2. Cell viability and morphology of hMSCs grown on different substrates. Cells are stained with DAPI (blue) and Calcein AM (green). (a) Graph showing cell viability in percentage normalized to coverslips used as reference. (Inset) Morphology of hMSCs grown on standard coverslips. (b–e) hMSCs grown on glass slide, Si/SiO_2, PET, and PDMS without graphene. (f–i) hMSCs grown on graphene-coated glass slide, Si/SiO_2, PET, and PDMS. Scale bars are 100 μm.

Stem cell research with graphene has become feasible only with the recent availability of cheap, high-quality, continuous graphene sheets on a large scale.[17] Here we show that graphene provides a new type of biocompatible scaffold for stem cells. Remarkably, graphene accelerates cell differentiation even in the absence of commonly used additional growth factors such as BMP-2. Taking into consideration both the intrinsic mechanical properties of graphene and the striking results of this study, we envisage a functional role of this new material as a versatile platform for future biomedical applications in general and stem cell therapies in particular.

Large-scale graphene used in this study was synthesized by the chemical vapor deposition method on copper foils. After growth, copper was etched and the same batch of graphene was transferred to four distinct substrates used in this study according to methods discussed elsewhere.[18] We studied the influence of graphene on stem cell growth by investigating four substrates with widely varying stiffness and surface roughness: (1) polydimethylsiloxane (PDMS), (2) polyethylene terephthalate (PET), (3) glass slide, and (4) silicon wafer with 300 nm SiO_2 (Si/SiO_2) (Figure S1 Table S1 in Supporting Information). Plain coverslips without graphene were used as a control or reference for normalization. Atomic force microscopy (AFM) was used to analyze the surface roughness of the various substrates with and without graphene coating. Transferred to PET, PDMS, and Si/SiO_2, the graphene sheet exhibits nanoripples with high density (Figure 1a,c,d) compared to graphene on glass slide (Figure 1a,b). Despite being only one atom thick, on Si/SiO_2 substrates with well-defined oxide thickness, graphene can be easily seen with a simple conventional optical microscope (Figure 1e). Therefore, detailed studies such as the evolution of cell differentiation with time were done mainly on graphene-coated Si/SiO_2 substrates. Two distinct sets of experiments were performed. First, cell viability was studied with cells cultured in normal stem cell medium. Next, stem cell differentiation was examined in cells cultured on conventional osteogenic media.

RESULTS AND DISCUSSION

Cell Viability and Morphology. We first discuss cell morphology and viability by image analysis on all four substrates with and without graphene coverage when cells were cultured in normal stem cell media. From Figure 2a, we see that, independent of the substrate, there is no significant difference ($p > 0.05$) in cell viability between graphene-coated and uncoated substrates. We also performed MTT assays (Figure S2 in Supporting Information) to confirm the cell viability data. Again, regardless of the substrate, there was no difference ($p > 0.05$) between uncoated and graphene-coated substrates, demonstrating that cell growth was indeed not affected by the presence of graphene. Note that cell viability is lower on PET and PDMS independent of the presence of graphene.

A similar conclusion can be reached by just comparing cell morphology with and without graphene. In general, the presence of graphene (Figure 2f–i) did not influence the shape of the cells in comparison to uncoated substrates (Figure 2b–e). Mesenchymal stem cells maintained their spindle shape across glass slides and Si/SiO_2 after 15 days of incubation (Figure 2b,c,f,g). Here, stem cells presented the usual elongated structure with noticeable filopodia extensions and cellular propagation fronts. In the case of PET

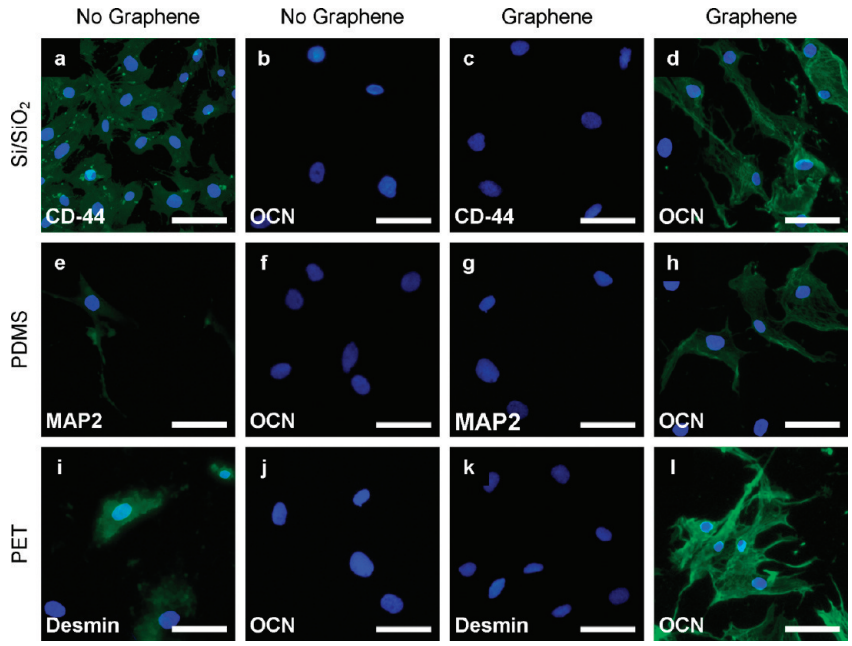

Figure 3. Immunostaining of cells growing on Si/SiO_2, PDMS, and PET without BMP-2 growth factor. Cells are stained with DAPI (blue) and either CD-44, MAP2, desmin, or osteocalcin (OCN) as indicated (green). (a–d) Cells growing on Si/SiO_2, without graphene showing presence of CD-44, and with graphene showing presence of OCN. (e–h) Cells growing on PDMS without graphene showing weak MAP2 immunostaining, and with graphene showing staining of OCN. (i–l) Cells growing on PET without graphene showing mild staining of desmin, and with graphene showing OCN immunostaining. Scale bars are 100 μm.

and PDMS, cells showed rounded or irregular morphology, most probably due to poor adhesion to the substrate (Figure 2d,e,h,i). This suggests that graphene does not hamper the normal growth of stem cells and that the incorporation of this material in implants or injured tissues would not affect the physiological conditions of the microenvironment. In fact, Raman measurements and visual inspection of the samples after cell incubation and subsequent removal clearly showed that the graphene sheets remained largely intact (Figure S5 in Supporting Information).

hMSCs Differentiation into Osteogenic Lineages. Next, specific markers were used to determine the conversion of hMSCs into specific cell types when cultured in osteogenic media. Note that conventional osteogenic medium does contain dexamethasone, which can lead to osteogenic differentiation by itself. However, it is usually administered in combination with other agents and growth factors such as BMP-2 to achieve differentiation through a synergistic effect. In none of the uncoated substrates studied here, the osteogenic medium alone was sufficient to lead to osteogenic differentiation over the whole duration of the experiment (15 days). In the absence of graphene, stem cells on coverslips (not shown), on glass slides (not shown), and on Si/SiO_2 (Figure 3a,b) did not differentiate: this was demonstrated by immunofluorescent staining of two typical protein markers, namely, CD-44 for hMSCs and osteocalcin (OCN) for osteoblasts. These three substrates showed a CD-44-positive staining and the absence of OCN. However, once these stiff substrates were coated with graphene, hMSCs lost their ability to bind the fluorescent antibody specific for CD-44 expression, suggesting they underwent a different fate (Figure 3c). In fact, hMSCs immunostained for OCN (Figure 3d) indicated osteogenic differentiation. On uncoated PDMS, hMSCs did not stain CD-44 but they showed a weak expression of MAP2 (typical neuronal marker, Figure 3e). On the other hand, in the case of uncoated PET, desmin (D33, a muscle cell marker) staining but not CD-44 was observed (Figure 3i). However, once coated with graphene, hMSCs growing also on these softer substrates bound specifically to OCN (Figure 3h,l) only, demonstrating that graphene is the driving force of bone cell formation, regardless of the underlying substrate.

This is most clearly seen in Figure 4b, showing the immunofluorescent staining of cells on a Si/SiO_2 wafer, which are cultured in osteogenic medium but only partially covered by graphene. Despite the stiffness of the substrate, specific immunostaining for OCN was only observed in the area covered by graphene. The boundary separating the graphene-coated region from the uncoated region is clearly visible even from the immunofluorescent image. These qualitative observations have been confirmed by quantitative alizarin red staining (Figure 4c,d), which indicates the presence or absence of calcium deposits due to bone nodule formation. The results for all substrates are summarized in Figure 4c, where we compared the extent of calcium deposition on each substrate, with and without graphene coating, in the absence of the typical growth

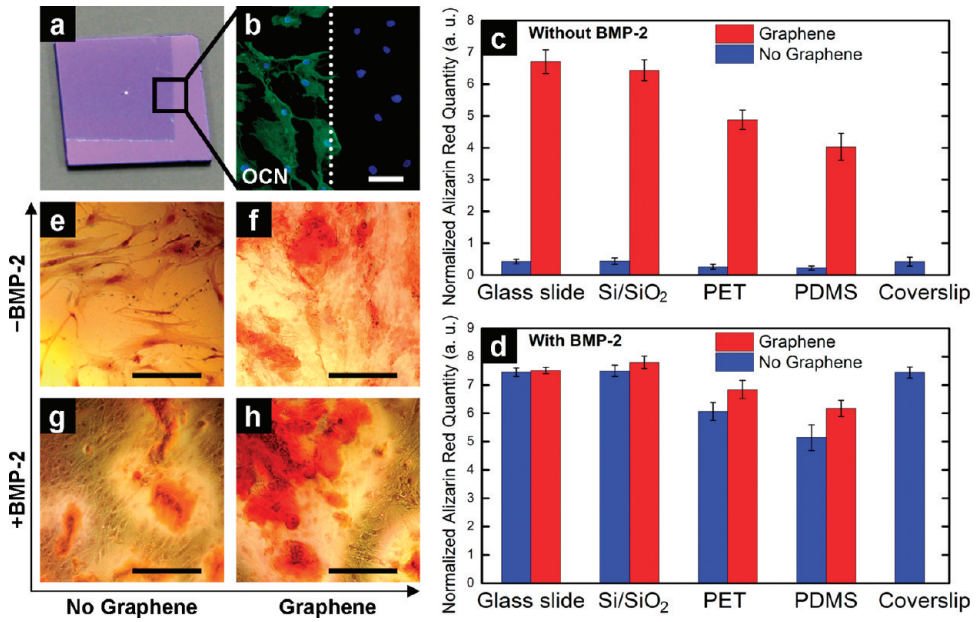

Figure 4. Graphene accelerates osteogenic differentiation. (a) Optical image of 1 cm × 1 cm, partially graphene-coated Si/SiO_2 chip, showing the graphene boundary. (b) Osteocalcin (OCN) marker showing bone cell formation on the same chip only on the graphene-coated area; the graphene boundary is also clearly visible here. (c,d) Alizarin red quantification deriving from hMSCs grown for 15 days on substrates with/without graphene. (c) Cells grown in the absence of BMP-2. Control with coverslips is shown as a reference. (d) Cells grown in the presence of BMP-2. Conventional plain coverslips were used as a positive control. (e−h) PET substrate stained with alizarin red showing calcium deposits due to osteogenesis. (e) PET without BMP-2 and without graphene; (f) PET without BMP-2 and with graphene; (g) PET with BMP-2 and without graphene; (h) PET with both BMP-2 and graphene. Scale bars are 100 μm.

factor BMP-2. A strong increase in calcium deposit with graphene coating is observed for all substrates. While the effect is more pronounced with the stiffer substrates, surprisingly graphene had a similar effect also on the softer substrates PET and PDMS. It should be noted that in the absence of growth factors both PDMS and PET are known to be less favorable toward osteoblasts.[7] Yet the presence of graphene induced a drastic change of their natural behavior similar to what has been observed with apatite coating on such polymers.[19−21] We would like to emphasize that also here the osteogenic medium alone was not sufficient to induce differentiation: within the 15 day time frame of the experiment, the control represented by coverslips in osteogenic medium *without* graphene (*i.e.*, hMSC cultured on ordinary tissue culture plate) did not show any calcium deposition. The evaluation of a separate set of samples by fluorescent-activated cell sorting (FACS) further supported our findings that graphene does accelerate the osteogenic differentiation of stem cells (Figure S3 in Supporting Information).

The impact of graphene on softer substrates such as PET became even more evident in a parallel study, in which we directly compared graphene's influence to that of BMP-2 (Figure 4e−h) after 15 days of incubation. In the absence of both graphene and BMP-2, no bone nodule formation was observed, as indicated by negative alizarin red staining (Figure 4e). As expected, we see positive staining with identical samples after the addition of BMP-2 (Figure 4g). On the other hand, graphene-coated PET showed a positive staining even without BMP-2 (Figure 4f). We also performed experiments where we combined both graphene coating and BMP-2 treatment (Figure 4h). In the case of PET and PDMS, we observed a significant enhancement of calcium deposits compared to the above-mentioned samples, which were either only coated with graphene or only treated with BMP-2. This enhancement was specific to soft substrates and much less evident on the stiffer glass slides and Si/SiO_2. Finally, quantitative alizarin red staining was used to study the role of graphene in the presence of BMP-2 (Figure 4d) for all four substrates. On the stiffer substrates (*i.e.*, glass slide and Si/SiO_2), the additional presence of graphene did not further enhance the production of calcium deposits ($p > 0.05$); calcium deposits had almost saturated purely from BMP-2. On the other hand, a clear, statistically significant increase ($p < 0.005$) is seen on the softer materials PET and PDMS. This again suggests that graphene itself has a remarkable role in the differentiation of hMSCs toward the osteogenic lineage.

Time-Dependent Study of Differentiation. An important parameter for practical applications is also the time a material takes to induce bone cell differentiation. To that purpose we studied how fast cells on graphene-coated Si/SiO_2 substrates differentiate over a time frame of 15 days in comparison to cells growing on uncoated Si/SiO_2 but treated with BMP-2. We studied

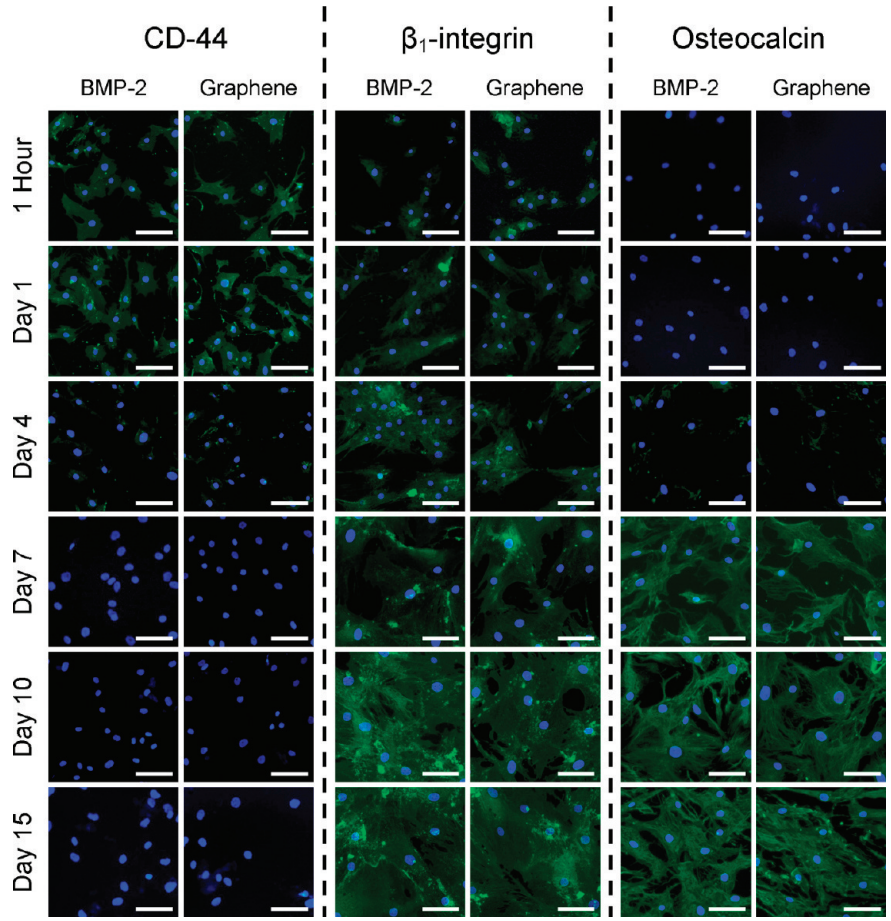

Figure 5. Immunostaining of cells growing on Si/SiO_2 substrates either treated with BMP-2 or coated with graphene. Experiments were performed from 1 h to 15 days. (Left) CD-44, marker for stem cells, decreased over time and completely disappeared by day 7. (Center) β1-integrin, marker for cell−substrate adhesion, increased over time, reaching its peak by day 15. (Right) OCN, marker for bone cells, became visible at day 4 and very intense by day 7. Scale bars are 100 μm.

these samples at specific time points of 1 h and 4, 7, 10, and 15 days (Figure 5). Interestingly, both BMP-2-treated and graphene-coated substrates were able to induce cell differentiation at the same rate. More precisely, hMSCs on neither substrate showed any sign of osteoblast formation until day 4. This is demonstrated by the intensity of fluorescence due to CD-44 marker, which is characteristic for stem cells and clearly visible already after 1 h of incubation. Conversely, fluorescence due to CD-44 decreased remarkably by day 4 and completely disappeared by day 7. On the other hand, a progressive enhancement of fluorescence was observed due to OCN (indication of terminal osteogenic differentiation) and β_1-integrin, a protein indicating cell−substrate interaction. The results confirmed a successful differentiation into bone cells with a strong adhesion to the substrates by day 7 for both types of samples. Si/SiO_2 substrates treated with (a) only BMP-2 and (b) only graphene were able to accelerate cell differentiation at the same rate over a period of 15 days of incubation (Figure 5). Equally important, in contrast to graphene, BMP-2 needed to be administered every 3 days during the course of the experiment due to the very short half-lives of BMP-2,[22,23] again showing graphene as a worthy replacement of biochemical growth factors.

Control Experiments. To confirm that graphene is critical for the observed stem cell differentiation, we performed control experiments with both amorphous carbon thin films and highly oriented pyrolytic graphite (HOPG) samples. Following identical experimental protocols, we observed that, while both types of samples did support cell proliferation, none of them led to cell differentiation (Figure 6d,f and Figure S4 in Supporting Information). Here we discuss the HOPG results in more detail. The results on amorphous carbon thin films are summarized in Supporting Information.

The AFM images of graphene and HOPG (Figure 6a, b) clearly show the difference in their topography. Cells were cultured on graphene or HOPG in osteogenic medium. After 4 days, the fluorescence deriving from the antibody specific for CD-44 expression was significantly lower for cells grown on graphene (Figure 6c) than for cells on HOPG (Figure 6d). At the same time, specific immunostaining for OCN is already detectable

with cells grown on graphene (Figure 6e), while only the DAPI-stained nuclei are visible for cells on HOPG (Figure 6f).

It is rather remarkable that a single continuous sheet of carbon atoms can strongly accelerate bone cell differentiation. The observed effect is almost certainly due to a complex interplay of mechanical, chemical, and electrical properties of graphene and the interactions between graphene and cells, as well as graphene and supporting substrates. This makes it difficult to identify the microscopic origin of the effect. However, a comparison with related CNT-based experiments does offer some clues (see Supporting Information). In addition, control experiments with amorphous carbon thin films and HOPG samples do provide some insights. In particular, the disparities between the results obtained with graphene and HOPG point toward mechanical properties and surface morphology as the decisive factors. While locally (~100 nm) the two systems have comparable surface morphology, on a larger scale, they look very different. CVD graphene consists of many ripples and wrinkles on the micrometer scale (Figure 6a). Such localized out-of-plane deformations are completely absent in HOPG graphite, the surface of which consists instead of a large number of micrometer size terraces (Figure 6b).

The correlation of cell morphology and substrate morphology has been investigated by several groups. Dulgar-Tulloch *et al.*[24] cultured hMSCs on ceramics with varying grain sizes between 24 and 1500 nm, showing that the 200 nm grain size was most favorable for hMSC proliferation independent of the surface chemistry, the surface roughness, and the crystal phase. Oh *et al.*[9] studied hMSCs on various diameters of TiO_2 nanotubes and observed a decrease in adhesion but an increase in osteogenic differentiation with increasing nanotube diameter. This is in good agreement with cell-morphology-induced differentiation observed by McBeath *et al.*[25] Even nanoscale patterning of poly(methyl methacrylate) (PMMA) has been reported to induce bone cell differentiation. Surprisingly, cell differentiation mainly took place when the nanopit arrays were disordered.[8] While the microscopic origins of these effects are not yet fully understood, it is worth noting that the topography of CVD graphene with its many ripples and wrinkles does mimic the disordered nanopit array of Dalby *et al.*[8] (Figure 6a). Such ripples and wrinkles are intrinsic to CVD graphene and originate from the difference in the thermal expansion coefficient of Cu and graphene.[18] Similarly to Dalby *et al.*,[8] the large-scale disorder in CVD graphene could play a role in protein adsorption, cell adhesion, proliferation, and differentiation. The ripples themselves also provide local curvature and, hence, could further enhance the reactivity of such graphene sheets.

Cell differentiation depends strongly also on substrate stiffness[26] and strain, such that when applied

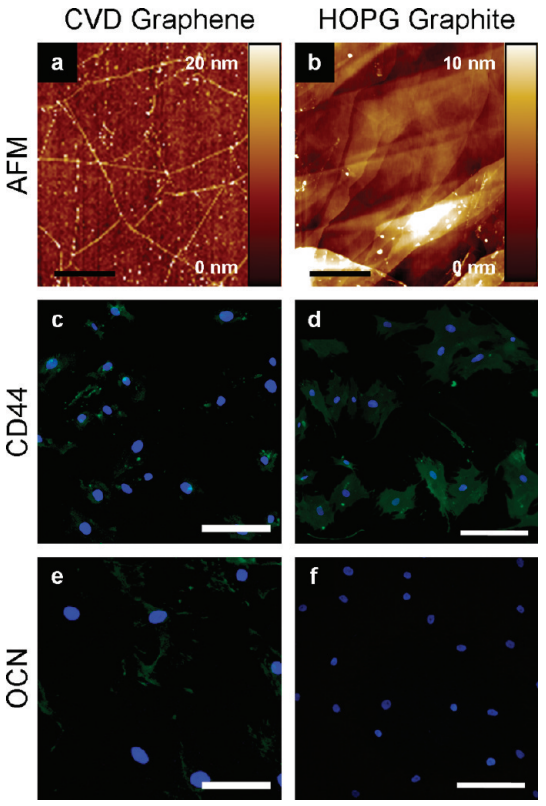

Figure 6. Comparison of osteogenic differentiation of hMSCs after 4 days on graphene-coated Si/SiO_2 and HOPG on coverslips. AFM images of (a) graphene and (b) HOPG. Scale bars are 5 μm. (c,d) Immunostating of CD-44 (green) on graphene and HOPG, respectively. (e,f) Immunostaining of OCN (green) on graphene and HOPG, respectively. Nucleus is stained with DAPI (blue). Scale bars are 100 μm.

(cyclically) it increases the expression of osteogenic markers for osteopontin (OPN) and BMP-2.[27,28] Therefore, graphene's exceptionally high Young's modulus[15] and its remarkable flexibility for out-of-plane deformation could also contribute to stem cell differentiation. However, we expect a significant influence of graphene's Young's modulus only with substrates that are much thinner and softer than those used in our studies. Even in the case of the PDMS substrates, the presence of graphene will only marginally increase its Young's modulus. On the other hand, the ability of graphene to sustain lateral stress could play a more important role in the context of providing just the right amount of local cytoskeletal tension. Together with the observation that graphene allows for easy out-of-plane deformation, this may lead to the formation of strong anchor points of the cytoskeleton. Such tension may allow for the unfolding of the mechanically sensitive protein of interest and change conformation.[6] Such forces could potentially be even easier to realize on PET and PDMS substrates since on these materials graphene is already prestrained.[29] Cell-induced out-of-plane deformations could further enhance the reactivity of nanorippled graphene sheets.

The fact that (HOPG) graphite is made out of weakly bound graphene planes may be equally important. In the presence of lateral forces, such materials easily shear off and are, therefore, commonly used in lubricants. In the specific context of cell adhesion and in view of the (lateral) contractual forces that cells exert on the surface, this effect may hamper strong cell adhesion. Note that cells can mechanically "sense" lower lying layers down to several tens of micrometers. In the case of graphene, the cells sense the underlying (amorphous) substrate instead.

CONCLUSIONS

To summarize, the presence of graphene did not influence the shape and the growth of the cells in normal stem cell media, demonstrating biocompatibility and suggesting that the incorporation of this material in implants or injured tissues would not affect the physiological conditions of the microenvironment. In the presence of an osteogenic medium, graphene coating helped by remarkably accelerating the differentiation of hMSCs at a rate comparable to differentiation under the influence of BMP-2. This represents a critical aspect to its successful use for stem-cell-based regenerative medicine strategies. In contrast to other substrates, graphene is neither brittle nor does it require further nanoscale patterning or functionalization. In addition, it is scalable and provides a cost-effective way to prepare scaffolds for biological tissues. Currently, graphene is only available in the form of sheets, and we envision a promising role of graphene located between implants and the surrounding tissues. However, the conditions under which graphene is grown are being constantly improved. There is, for example, a strong effort to establish graphene growth at much lower temperatures. Thus, growth on alternative biocompatible and biodegradable surfaces, potentially even without the need to resort to catalytic metal films, seems feasible. Even growth on 3D scaffolds have recently been demonstrated.[30]

METHODS

Substrate Preparation. Graphene was grown on copper foils by chemical vapor deposition at 1000 °C in a mixture of hydrogen and methane as discussed elsewhere.[18] The graphene film was mechanically supported by a thin film of PMMA (Microchem), and the copper foil was etched in a weak solution of ammonium persulfate (Sigma). The graphene coated with PMMA was transferred to deionized water to remove residues, and the transfer was completed by gently contacting graphene with the substrate and lifting it out of the water. To avoid any residues from the transfer process, the samples were left in warm acetone for 12 h followed by 3 h in isopropyl alcohol. In a final step, the Si/SiO_2 substrates were annealed in Ar/H_2 90/10 wt % for 7 h at 300 °C to further reduce impurities in the graphene layer. However, note that Si/SiO_2 without the additional step of annealing showed the same cell viability and induced stem cell differentiation at the same rate (data not shown).

Cell Lines and Markers. Human mesenchymal stem cells (hMSCs) were purchased from ATCC and cultured in low-glucose Dulbecco's modified eagle medium (Sigma) supplemented with 10% FBS (Invitrogen), 1% penicillin/streptomycin (Gibco), 1% non-essential amino acids (Sigma), and 1% sodium pyruvate (Sigma). The hMSCs at passage 2 were used in this study. Osteogenic medium consisting of DMEM basal medium (Sigma) added with dexamethasone, L-glutamine, ascorbic acid, and β-glycerophosphate was prepared according to a known procedure.[31] FITC goat anti-mouse antibody was purchased from Biolegend, San Diego, California (USA). Markers (osteocalcin (OCN), CD44, desmin (D33), MAP-2, β_1-integrin) were purchased from Acris Antibodies GmbH (Germany).

Cell Viability. The hMSCs (20 000 cells/well, 24-well plate) were seeded on uncoated (control) and graphene-coated (test) chips and cultured in normal stem cell medium. Post-confluence (2 weeks), cells growing on each chip were transferred to a new well plate and washed three times with 2 mL of PBS. One milliliter of PBS was added to each well followed by 5 μL of 1 mM calcein acetoxymethyl ester (calcein AM) and incubated at room temperature for 15 min. After removing the unbound stains, the chips were inverted onto glass slides mounted with Vectashield with DAPI (H 1200, Vector Laboratories) and visualized under a fluorescence microscope (Nikon AZ-100 multipurpose microscope). Pictures were taken at 4 different positions of the chips and processed by ImageJ software to count the number of viable cells to the number of nucleus as determined by staining with DAPI. Cell viability was measured by comparing the cell numbers for each substrate with the cells counted on coverslips. In addition, (3-(4,5-dimethylthiazol-2-yl)-2,5-diphenyltetrazolium)bromide (MTT) assays were carried out, in which cytotoxicity evaluation was based on the activity of enzymes to reduce MTT to formazan dyes, giving a purple color.[32] Experiments were carried out in triplicate, following the procedure reported in the supporting document. The morphology of the hMSCs on different substrates was compared according to the image as seen in the form of calcein AM staining.

Alizarin Red Staining and Quantification. The hMSCs (20 000 cells/well, 24-well plate) were seeded into the control and the test well plate. After 24 h, osteogenesis was induced by replacing the original medium with osteogenic medium, which was changed every 3 days up to confluence (2 weeks).

Alizarin red staining was performed using the protocol adapted from Chemicon mesenchymal stem cell osteogeneis kit (Cat. No. SCR028). Briefly, the medium was aspirated out from each well, and cells were fixed with ice cold 70% ethanol for 1 h at room temperature. Then the cells were rinsed twice with Milli-Q water followed by addition of 2 mL of alizarin red (Sigma) solution for each well and incubated for 30 min. Finally, the unstained alizarin red was washed with Milli-Q water, and the chips were visualized under a microscope (Nikon Eclipse TE2000-U, Japan). Cells with calcium deposits due to bone nodule formation were stained red. Alizarin red quantification was done using a previously reported procedure.[33]

Immunofluorescence of hMSCs and Time-Dependent Differentiation Study. The hMSCs at 20 000 cells/well (24-well plate) were seeded, osteoinduced, and incubated up to confluence (2 weeks) as reported above. The cells on all of the chips were fixed by treating them with ice cold 50%/50% methanol/acetone. After 5 min, methanol/acetone was removed and the chips were left open inside the laminar hood to be air-dried. After the chips were completely dried, the fixed cells were treated with 10% FBS (blocking agent) in PBS for 20 min. The blocking agent was aspirated out, and 5 μL of different antibodies to cellular markers (CD-44 for hMSCs, OCN for osteoblasts, desmin for

muscle cells, and MAP2 for neuronal cells) was added onto separate chips (previously marked). After 1 h, the cells on the chips were extensively washed in Milli-Q water for 5 min and then rinsed in PBS 1× for 5 min. After that, 100 μL of diluted (1/100) FITC goat anti-mouse antibody was added on to each chip and incubated at room temperature. After 30 min, the cells were washed with Milli-Q water for 5 min and then rinsed in PBS 1× for 5 min. The chips were inverted onto glass slides mounted with Vectashield with DAPI (H 1200, Vector Laboratories) and visualized under a fluorescence microscope (Nikon AZ-100 multipurpose microscope).

For time-dependent differentiation experiment, osteogenic differentiation was further evaluated over a time frame of 2 weeks. Uncoated substrates were subjected to BMP-2 (75 ng/mL, added every 3 days) and compared to graphene-coated substrates at 1 h and at days 1, 4, 7, 10, and 15 in terms of binding to CD-44 (which stains hMSCs), β_1-integrin (which indicates cell−substrate adhesion), and OCN (which indicates bone cells). The above-mentioned procedure was followed for the immunofluorescence and imaging purposes.

Acknowledgment. B.Ö. acknowledges support by the Singapore National Research Foundation under NRF RF Award No. NRFRF2008-07, and A*STAR SERC TSRP-Integrated Nano-Photo-Bio Interface (R-144-000-275-305) and by NUS NanoCore. G. P. acknowledges the A*STAR SERC TSRP - Integrated Nano-Photo-Bio Interface Award and the Singapore Bioimaging Consortium, Nikon Imaging Centre, for providing technical assistance and microscope facilities. B.H.H. acknowledges support by the National Research Foundation of Korea (NRF) funded by the Ministry of Education, Science and Technology (2010-0028075, 2010-0081966, 2011-0006268).

Supporting Information Available: Sample characterization, MTT assay, amorphous carbon discussion. This material is available free of charge *via* the Internet at http://pubs.acs.org.

REFERENCES AND NOTES

1. Spradling, A.; Drummond-Barbosa, D.; Kai, T. Stem Cells Find Their Niche. *Nature* **2001**, *414*, 98–104.
2. Lutolf, M. P.; Hubbell, J. A. Synthetic Biomaterials as Instructive Extracellular Microenvironments for Morphogenesis in Tissue Engineering. *Nat. Biotechnol.* **2005**, *23*, 47–55.
3. Discher, D. E.; Mooney, D. J.; Zandstra, P. W. Growth Factors, Matrices, and Forces Combine and Control Stem Cells. *Science* **2009**, *324*, 1673–1677.
4. Jaiswal, N.; Haynesworth, S. E.; Caplan, A. I.; Bruder, S. P. Osteogenic Differentiation of Purified, Culture-Expanded Human Mesenchymal Stem Cells *In Vitro*. *J. Cell Biochem.* **1997**, *64*, 295–312.
5. Engler, A. J.; Sen, S.; Sweeney, H. L.; Discher, D. E. Matrix Elasticity Directs Stem Cell Lineage Specification. *Cell* **2006**, *126*, 677–689.
6. Reilly, G. C.; Engler, A. J. Intrinsic Extracellular Matrix Properties Regulate Stem Cell Differentiation. *J. Biomech.* **2010**, *43*, 55–62.
7. Kim, S. J.; Lee, J. K.; Kim, J. W.; Jung, J. W.; Seo, K.; Park, S. B.; Roh, K. H.; Lee, S. R.; Hong, Y. H.; Kim, S. J.*et al.* Surface Modification of Polydimethylsiloxane (PDMS) Induced Proliferation and Neural-like Cells Differentiation of Umbilical Cord Blood-Derived Mesenchymal Stem Cells. *J. Mater. Sci: Mater. Med.* **2008**, *19*, 2953–2962.
8. Dalby, M. J.; Gadegaard, N.; Tare, R.; Andar, A.; Riehle, M. O.; Herzyk, P.; Wilkinson, C. D. W.; Oreffo, R. O. C. The Control of Human Mesenchymal Cell Differentiation Using Nanoscale Symmetry and Disorder. *Nat. Mater.* **2007**, *6*, 997–1003.
9. Oh, S.; Brammer, K. S.; Li, Y. S. J.; Teng, D.; Engler, A. J.; Chien, S.; Jin, S. Stem Cell Fate Dictated Solely by Altered Nanotube Dimension. *Proc. Natl. Acad. Sci. U.S.A.* **2009**, *106*, 2130–2135.
10. Nayak, T. R.; Jian, L.; Phua, L. C.; H o, H. K.; Ren, Y.; Pastorin, G. Thin Films of Functionalized Multiwalled Carbon Nanotubes as Suitable Scaffold Materials for Stem Cells Proliferation and Bone Formation. *ACS Nano* **2010**, *4*, 7717–7725.
11. Konttinen, Y. T.; Zhao, D.; Beklen, A.; Ma, G.; Takagi, M.; Kivelä-Rajamäki, M.; Ashammakhi, N.; Santavirta, S. The Microenvironment around Total Hip Replacement Prostheses. *Clin. Orthop. Relat. Res.* **2005**, *430*, 28–38.
12. Novoselov, K. S.; Geim, A. K.; Morozov, S. V.; Jiang, D.; Zhang, Y.; Dubonos, S. V.; Grigorieva, I. V.; Firsov, A. A. Electric Field Effect in Atomically Thin Carbon Films. *Science* **2004**, *306*, 666–669.
13. Geim, A. K. Graphene: Status and Prospects. *Science* **2009**, *324*, 1530–1534.
14. Frank, I. W.; Tanenbaum, D. M.; van der Zande, A. M.; McEuen, P. L. Mechanical Properties of Suspended Graphene Sheets. *J. Vac. Sci. Technol., B* **2007**, *25*, 2558–2561.
15. Lee, C.; Wei, X.; Kysar, J. W.; Hone, J. Measurement of the Elastic Properties and Intrinsic Strength of Monolayer Graphene. *Science* **2008**, *321*, 385–388.
16. Lee, Y.; Bae, S.; Jang, H.; Jang, S.; Zhu, S.-E.; Sim, S. H.; Song, Y. I.; Hong, B. H.; Ahn, J.-H. Wafer-Scale Synthesis and Transfer of Graphene Films. *Nano Lett.* **2010**, *10*, 490–493.
17. Bae, S.; Kim, H.; Lee, Y.; Xu, X.; Park, J. S.; Zheng, Y.; Balakrishnan, J.; Lei, T.; Kim, H. R.; Song, Y. I.*et al.* Roll-to-Roll Production of 30-Inch Graphene Films for Transparent Electrodes. *Nat. Nanotechnol.* **2010**, *5*, 574–578.
18. Li, X.; Cai, W.; An, J.; Kim, S.; Nah, J.; Yang, D.; Piner, R.; Velamakanni, A.; Jung, I.; Tutuc, E.*et al.* Large-Area Synthesis of High-Quality and Uniform Graphene Films on Copper Foils. *Science* **2009**, *324*, 1312–1314.
19. Kawai, T.; Ohtsuki, C.; Kamitakahara, M.; Miyazaki, T.; Tanihara, M.; Sakaguchi, Y.; Konagaya, S. Coating of an Apatite Layer on Polyamide Films Containing Sulfonic Groups by a Biomimetic Process. *Biomaterials* **2004**, *25*, 4529–4534.
20. Kim, H.-M.; Kishimoto, K.; Miyaji, F.; Kokubo, T.; Yao, T.; Suetsugu, Y. Composition and Structure of Apatite Formed on Organic Polymer in Simulated Body Fluid with a High Content of Carbonate Ion. *J. Mater. Sci. Mater. Med.* **2000**, *11*, 421–426.
21. Kim, H.-M.; Kishimoto, K.; Miyaji, F.; Kokubo, T.; Yao, T.; Suetsugu, Y.; Tanaka, J.; Nakamura, T. Composition and Structure of the Apatite Formed on PET Substrates in SBF Modified with Various Ionic Activity Products. *J. Biomed. Mater. Res.* **1999**, *46*, 228–235.
22. Balmayor, E. R.; Feichtinger, G. A.; Azevedo, H. S.; van Griensven, M.; Reis, R. L. Starch-Poly-*N*′′-Caprolactone Microparticles Reduce the Needed Amount of BMP-2. *Clin. Orthop. Relat. Res.* **2009**, *467*, 3138–3148.
23. Dragoo, J. L.; Choi, J. Y.; Lieberman, J. R.; Huang, J.; Zuk, P. A.; Zhang, J.; Hedrick, M. H.; Benhaim, P. Bone Induction by BMP-2 Transduced Stem Cells Derived from Human Fat. *J. Orthop. Res.* **2003**, *21*, 622–629.
24. Dulgar-Tulloch, A. J.; Bizios, R.; Siegel, R. W. Human Mesenchymal Stem Cell Adhesion and Proliferation in Response to Ceramic Chemistry and Nanoscale Topography. *J. Biomed. Mater. Res. A* **2008**, *90A*, 586–594.
25. McBeath, R.; Pirone, D. M.; Nelson, C. M.; Bhadriraju, K.; Chen, C. S. Cell Shape, Cytoskeletal Tension, and RhoA Regulate Stem Cell Lineage Commitment. *Dev. Cell.* **2004**, *6*, 483–495.
26. Discher, D. E.; Janmey, P.; Wang, Y.-L. Tissue Cells Feel and Respond to the Stiffness of Their Substrate. *Science* **2005**, *310*, 1139–1143.
27. Jang, J.-Y.; Lee, S. W.; Park, S. H.; Shin, J. W.; Mun, J. W.; Kim, S.-H.; Kim, D. H.; Shin, J.-W. Combined Effects of Surface Morphology and Mechanical Straining Magnitudes on the Differentiation of Mesenchymal Stem Cells without Using Biochemical Reagents. *J. Biomed. Biotechnol.* 2011, doi: 10.1155/2011/860652.
28. Rui, Y. F.; Lui, P. P. Y.; Ni, M.; Chan, L. S.; Lee, Y. W.; Chan, K. M. Mechanical Loading Increased BMP-2 Expression Which Promoted Osteogenic Differentiation of Tendon-Derived Stem Cells. *J. Orthop. Res.* **2011**, *29*, 390–396.
29. Ni, Z. H.; Yu, T.; Lu, Y. H.; Wang, Y. Y.; Feng, Y. P.; Shen, Z. X. Uniaxial Strain on Graphene: Raman Spectroscopy

Study and Band-Gap Opening. *ACS Nano* **2008**, *2*, 2301–2305.
30. Chen, Z.; Ren, W.;Gao, L.; Liu, B.; Pei, S.; Cheng, H.-M. Three-Dimensional Flexible and Conductive Interconnected Graphene Networks Grown by Chemical Vapour Deposition. *Nat. Mater.* 2011, doi: 10.1038/nmat3001.
31. Fahmi, H.; Pelletier, J.-P.; Mineau, F.; Martel-Pelletier, J. 15d-PGJ_2 Is Acting as a `Dual Agent' on the Regulation of COX-2 Expression in Human Osteoarthritic Chondrocytes. *Osteoarthritis Cartilage* **2002**, *10*, 845–848.
32. Mosmann, T. Rapid Colorimetric Assay for Cellular Growth and Survival: Application to Proliferation and Cytotoxicity Assays. *J. Immun. Met.* **1983**, *65*, 55–63.
33. Tataria, M.; Quarto, N.; Longaker, M. T.; Sylvester, K. G. Absence of the p53 Tumor Suppressor Gene Promotes Osteogenesis in Mesenchymal Stem Cells. *J. Pediatr. Surg.* **2006**, *41*, 624–632.